

## Optimization of imaging geometry in x-ray microtomography system

Sunyoung Jang, Hanbean Youn, Ho Kyung Kim\*

School of Mechanical Engineering, Pusan National University, Busan 609-735, South Korea

\*Correspondence: hokyung@pusan.ac.kr

### 1. Introduction

Cone-beam computed tomography (CBCT) is useful to histologically monitor medicinal and pathological effects in body without subject manipulation and/or sacrifice. This kind of study generally uses small animals as subject, such as rats or mice, to imitate human body. Hence, CBCT capable of high-resolution imaging is required, and we call this microtomography (simply, micro-CT).

Since imaging performance of micro-CT is directly connected to the reliability of the histological research, we suggest a guideline to optimize the performance of micro-CT systems by using ideal observer model.

Although many physical parameters affect the overall performance of micro-CT system, characteristic of an imaging detector is dominant. Using the cascaded model analysis, we obtain theoretical detective quantum efficiency (DQE), which represents the overall detector-system performance as a function of detector-system parameters [1]. And then, we simply extend it to generalized system DQE considering imaging geometry in micro-CT. Finally, ideal observer model is applied to the developed system DQE. Single descriptive value, known as the detection ability, of a target subject is investigated as a function various physical parameters affecting the imaging capability of a micro-CT.

### 2. Methods and Results

In order to express the characteristics of the micro-CT system in terms of DQE, various system parameters are first defined; (1) detector parameters: pixel pitch, and additive electronic noise, (2) source parameter: focal spot size  $a_{focal}$ , and (3) geometric parameters: source-to-detector  $d_{SD}$  and source-to-object (or subject) distances  $d_{SO}$ , and magnification factor  $M$ .

#### 2.1 System configuration

Fig. 1 schematically illustrates the imaging geometry of micro-CT considered in this study. The micro-CT system is composed of x-ray source, flat-panel detector and rotational stage. The detector is assumed as one based on indirect-conversion technology and it employs a fiber-optic plate (FOP) between the scintillator and the readout pixel array to avoid radiation damage in the pixel array.

#### 2.2 Detector and system DQEs

In general, DQE is calculated by measured modulation-transfer function (MTF) and noise-power spectrum (NPS). In this study, however, the detector

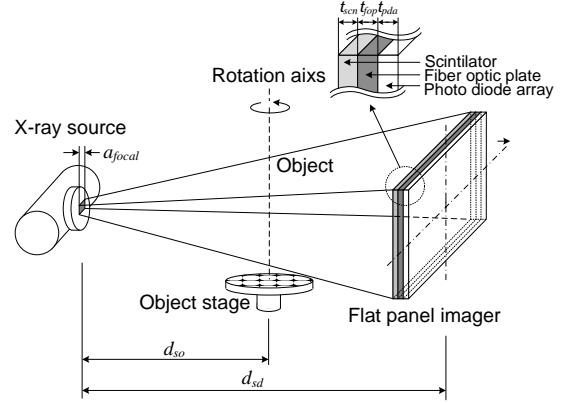


Fig. 1. Schematic illustration of the micro-CT system. Rotational stage is positioned between the x-ray source and the flat-panel imager (detector). The detector consists of a scintillator, a 3-mm-thick FOP and two-dimensional photo diode array.

DQE has been theoretically modeled by using linear cascaded system theory [2];

$$DQE_{det}(u') = \frac{\bar{g}_1 \bar{g}_2 \bar{g}_4 T_3^2(u') T_5^2(u')}{[1 + \bar{g}_4 (\bar{g}_2 + \varepsilon_g) T_3^2(u')] T_5^2(u') + \frac{S_{add}(u')}{a_{pd}^4 \bar{q}_0 \bar{g}_1 \bar{g}_2 \bar{g}_4}} \quad (1)$$

where  $\bar{g}_1$  denotes the quantum detection efficiency,  $\bar{g}_2$  secondary quantum gain,  $\bar{g}_4$  the coupling efficiency,  $T_3$  MTF of the scintillator,  $T_5$  MTF describing the pixel aperture,  $\varepsilon_g$  the Poisson excess of the quantum gain stage,  $S_{add}$  NPS due to the additive electronic noise,  $a_{pd}$  ( $= 144 \mu\text{m}$ ) pixel pitch, and  $\bar{q}_0$  x-ray photon fluence at the image plane. Most of these parameters were estimated by Monte Carlo methods [3]. Task size of 0.1 and 0.2 mm were considered for various focal spot sizes of, 0.1, 0.5 and 1.0 mm. X-ray spectrum was modeled as 2.5-mm-thick aluminum-filtered 40 kVp of tungsten target by using SRS-78(IPEM, UK) spectrum simulator.

The detector DQE does not contain the characteristics of the imaging geometry of micro-CT. Using the concept of "generalized DQE" [3], the detector DQE has been extended by accounting for magnification effect and focal spot blur. MTF of focal spot can be given by [1]

$$T_{focal}(u') = e^{-\pi[M-1]a_{focal}u'}^2 \quad (2)$$

Therefore, the system DQE becomes to

$$DQE(u') = T_{focal}^2\left(\frac{u'}{M}\right) DQE_{det}\left(\frac{u'}{M}\right) \quad (3)$$

#### 2.3 Detectability index

In order to contain effects of task size,  $a_{task}$ , task function is applied to the DQE formalism. Task function is object size in the frequency domain;

$$W_{task} = ke \frac{\pi a_{task}^2}{u^2} \quad (4)$$

Detectability is a single value and obtained from taking integration of the weighted DQE by the task function [4,5], and it is used for optimizing the system. Detectability includes both the effects of focal spot and object size on the imaging performance of detector. Therefore, it may be reasonable to use the detectability as figure of merit to estimate the entire system performance. Detectability index with respect to DQE,  $d_{DQE}$  is defined as

$$d_{DQE} = \int_0^{u'_{ny}} W_{task}^2(u') DQE(u') du' \quad (5)$$

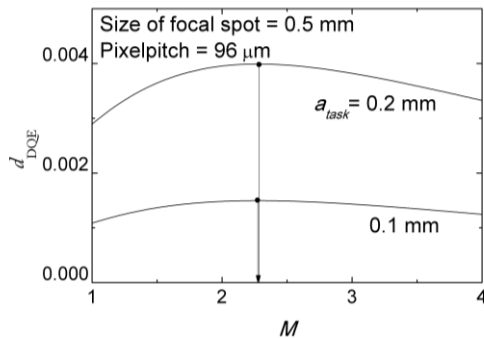


Fig. 2. Detectability as a function of magnification factor for different task sizes.

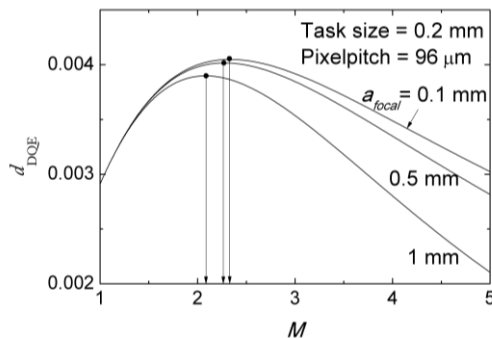


Fig. 3. Detectability as a function of magnification factor for different sizes of focal spot.

Fig. 2, 3 and 4 show detectabilities as a function of magnification factor with respect to task size, focal spot size, and pixel pitch, respectively. As shown in Fig. 2, small size of object improves detectability. The optimal magnification is almost insensitive to the task sizes. Task size is the dominant factor affecting detectability, because decrease in MTF is relatively less at the low-frequency region and the task size scales the MTF performance implicitly included in the DQE formalism. Fig. 3 shows that a larger focal spot size decreases the optimal magnification factor. Since blur becomes severer as the focal size increases, the detectability is much sensitive in high magnification. Fig. 4 shows that a smaller pixel pitch decreases optimal magnification since the small pixel pitch improves resolving power. Higher magnification provides higher spatial resolution, but the corresponding magnified focal-spot blur worsens the spatial resolution. Thus, optimal magnification can

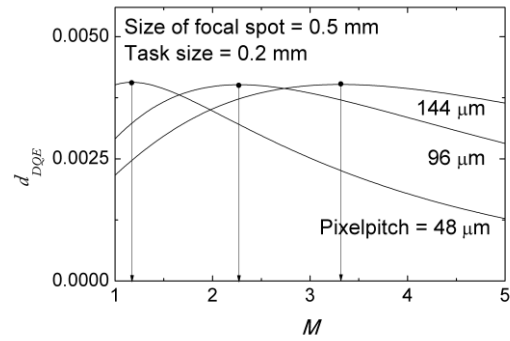


Fig. 4. Detectability as a function of magnification factor for different pixel pitches.

be achieved by trade-off between two opposite effects of the focal spot size and pixel pitch.

### 3. Conclusions

We have investigated the strategy of optimization of the imaging geometry of micro-CT in theoretical frameworks with respect to focal spot size, task size and detector pixel pitch. The results of this study imply that it could be possible to optimize the imaging geometry in restricted experimental conditions. It is expected that this study would be useful to modify or improve the conventional systems for better imaging capabilities. In the future, the influence of x-ray scatter should be incorporated in the model.

### ACKNOWLEDGEMENT

This work was supported by a Grant-in-Aid for Strategy Technology Development Programs from the Korea Ministry of Knowledge Economy (No. 10032060) and the Korea Research Foundation (KRF) Grant funded by the Korea government (MEST) (KRF-2008-313-D01339).

### REFERENCES

- [1] J. H. Siewerdsen and D.A. Jaffray, Optimization of x-ray imaging geometry (with specific application to flat-panel cone-beam computed tomography), *Med. Phys.* 27, 1903-1914, 2000
- [2] I. A. Cunningham, M.S. Westmore, and A. Fenster, A spatial-frequency dependent quantum accounting diagram and detective quantum efficiency model of signal and noise propagation in cascade imaging system, *Med. Phys.* 21, 417-427, 1994
- [3] S.J. Boyce and E. Samei, Imaging properties of digital magnification radiography, *Med. Phys.* 33, 984-996, 2006
- [4] International Commission on Radiation Units and Measurements Report No.54, *Med. Imag. the Assessment of image quality*, ICRU, Bethesda, MD, 1996
- [5] J. P. Bissonnette, I. A. Cunningham, and P. Munro, Optimal phosphor thickness for portal imaging, *Med. Phys.* 24, 803-814, 1997